Indonesian Journal of Electrical Engineering and Computer Science
Vol. 42, No. 3, June 2026, pp. 678~687
ISSN: 2502-4752, DOI: 10.11591/ijeecs.v42.i3.pp678-687

Enhancing the performance of 3-phase induction motors by developing a 40-degree asymmetrical coil design for the stator coil

Zuriman Anthony[1,2], Refdinal Nazir[2], Muhammad Imran Hamid[2]
[1]Department of Electrical Engineering, Faculty of Engineering, Institut Teknologi Padang, Padang, Indonesia
[2]Department of Electrical Engineering, Faculty of Engineering, Universitas Andalas, Padang, Indonesia

Article Info

Article history:

Received Dec 6, 2025
Revised Apr 2, 2026
Accepted May 26, 2026

Keywords:

2-layer coil design
Asymmetrical coil design
Induction motor coil
Performance enhancement
Stator coil design

ABSTRACT

The use of three-phase induction motors in industry is very widespread due to their durability, simplicity, cost, and ease of use. These motors are continuously developed to improve performance. However, the increase in motor performance is directly proportional to the increase in the motor's cost. Therefore, innovative solutions are needed to make three-phase induction motors more efficient without raising the motor's price. The study's goal is to create a motor coil design that won't cost a lot more but will make 3-phase induction motors more efficient. This study developed a 2-layer coil design with a pair of poles for each layer. The second coil layer is located 40 electrical degrees away from the first layer. In the lab, the motor's performance was assessed and compared to a conventional motor. This new motor uses identical materials as the conventional model; therefore, it does not incur additional costs. The results showed that this method could increase the rotor speed, output power, efficiency, and load torque of the motor by 0.21%, 16.29%, 15.90%, and 16.05%, respectively.

Corresponding Author:

Refdinal Nazir
Department of Electrical Engineering, Faculty of Engineering, Universitas Andalas
Limau Manis, Pauh, Padang City 25175, West Sumatra, Indonesia
Email: refdinalnazir@eng.unand.ac.id

1. INTRODUCTION

Three-phase induction motors are alternating current electric motors widely utilized in industry [1]-[12] due to their user-friendliness, robust build, affordability, dependability, ease of maintenance, and operating system [1], [2], [4]-[8], [11]. With this in mind, these motors are still being improved so that they work better and more efficiently [13]. The efficacy of 3-phase induction motors has been improved through the implementation of various techniques, such as the integration of permanent magnets into the rotor [6], [7], [14]; the fabrication of motor coils exceeding three phases and the provision of a power source adaptable to the number of phases [15]-[32] and the advancement of rotor slot [33] and motor coil configurations [34]-[39].

By adding solid magnets to the rotor [6], [7], [14], the induction motor will be stronger, move faster, and use its power more efficiently. Nonetheless, the issue lies in the fact that employing permanent magnets on the rotor incurs supplementary expenses for the acquisition of the utilized permanent magnets [6], [7], [14]. Higher quality permanent magnets utilized in the motor result in increased production costs.

The fabrication of motor coils exceeding three phases to 3-phase motor can make it more powerful [27], [28]; more efficient [32] and more powerful. But if you want to add more phases to the motor coil, you'll need to spend more money on a new power source [15]-[31], as well as a dependable control circuit and safety system [16], [20], [22], [23], [39]-[42]. Consequently, we must devise a novel approach to enhance the performance of 3-phase induction motors without incurring significant additional costs.

The paper suggests a new design for the stator coil to enhance the performance of 3-phase induction motors. This is because it is a cheap approach to make motors work better [32], [36]-[39]. The stator coils are constructed using a 40-degree asymmetric configuration, similar to the 40-degree asymmetric 6-phase coil design. The motor performance research only looks at experimental data from the lab. It focuses on how changes in load affect the coil current, speed, load torque, output power, and efficiency of the motor. The novel motor is contrasted with a traditional motor that has the same stator slots, coil turns per slot, and rotor and stator designs.

2. THE COMPREHENSIVE THEORETICAL BASIS

A three-phase induction motor comprises 3 identical coils that are 120º out of phase. This motor generally functions on a three-phase power supply that is 120 degrees phase-shifted. Figure 1 illustrates the coil layout design for the motor, with Figure 1(a) depicting the stator winding configuration for the 18-slot, two-pole induction motor and Figure 1(b) a basic vector representation of the winding distribution.

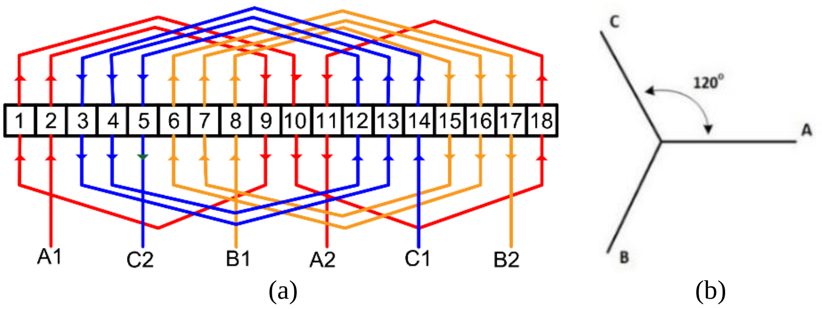

Figure 1. Coil layout design for a 3-phase motor within its slot (a) stator winding design for the 18-slot three-phase induction motor with two poles and (b) basic vector representation

A 6-phase induction motor comprises 6 coils and is deemed more reliable than a 3-phase induction motor owing to its capacity to operate with reduced vibration, increased stability, higher flux density, torque [27], [28], power [32], and improved efficiency. Figure 2 illustrates various variations of 6-phase winding designs. The coil design in Figure 2(a) is called a 3-phase dual design because the distance between the coils is 0º electricity, while the coil design in Figure 2(b) is called a symmetrical 6-phase coil design because the distance between the coils is 60º electricity, and the coil design in Figure 2(c) is referred to as an asymmetrical 6-phase coil design due to the unequal spacing between the coils; specifically, a_1 and a_2 are 30º electricity but the distance between coils a_2 and b_1 is 90º electricity.

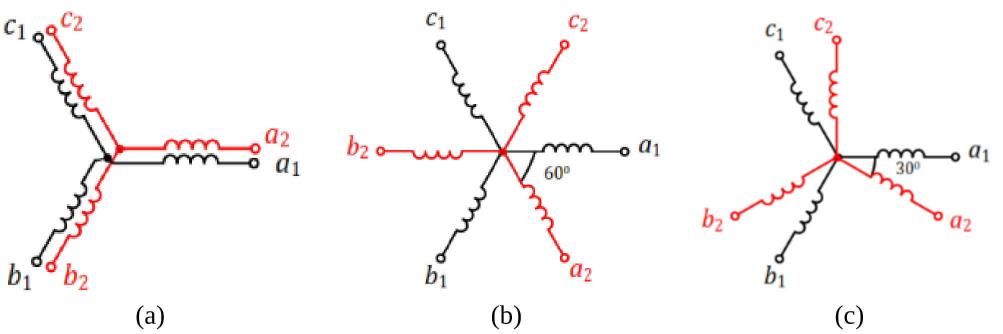

Figure 2. 6-phase winding design configurations include: (a) a 3-phase dual design (0º), (b) a 6-phase symmetrical design (60º), and (c) a 6-phase asymmetrical design (30º)

To guarantee operation at the specified speed, induction motor coils are frequently constructed with a predetermined number of poles [43]. The coils of an induction motor are designed according to these formulas to ensure it works [43].

$$Q_1 = {}^{s_1}\!/_{2p} \quad (1)$$

$$q_1 = {}^{s_1}\!/_{2p\, m_1} \quad (2)$$

$$\tau = Q_1 \quad (3)$$

$$y \leq Q_1 \quad (4)$$

$$\alpha_{el} = {}^{p\,360^o}\!/_{s_1} \quad (5)$$

Here, 'Q_1' stands for the quantity of slots in a single pole; 's_1' for the quantity of slots in the stator; 'p' for the quantity of pole pairs; 'q_1' for the quantity of slots in a single pole per phase; 'm_1' for the quantity of phases in the stator coil; 'τ' for the pitch of the pole; 'y' for the coil pitch; and 'α_{el}' for the size of the electrical angle between two neighboring slots.

The magnetic flux that is generated by the motor coil '∅' has a direct influence on the induced emf 'E_1' that is present in the coil as well as the performance of the motor. This influence can be explained by the equation that is presented below [44].

$$\emptyset = \tau\, L\, B_m\, 2/\pi \quad (6)$$

$$E_1 = 4{,}44\, f\, N_1\, k_{w1}\, \emptyset \quad (7)$$

In this case, 'B_m' is the maximum air gap flux density, 'L' is the stator stack length, 'k_{w1}' is the winding factor, 'N_1' is the turns quantity in the stator coil, and 'f' is the source frequency.

The rotor current observed from the stator perspective, denoted as 'I_2', can be determined using the subsequent equation [43]:

$$I_2 = {}^{E_1}\!\Big/_{\left(\frac{R_2}{s} + jX_2\right)} \quad (8)$$

In this instance, 's' represents the slip, 'X2' represents the inductive reactance, and 'R2' represents the rotor resistance observed from the stator.

Use these formulas to find a 3-phase induction motor's mechanical power (P_m), output power (P_{out}), load torque (T_L), rotor speed rotation (ω_r), input power (P_{in}), and efficiency (η) [43]:

$$P_m = 3\,(I_2)^2 \frac{R_2}{s}\,(1-s) \quad (9)$$

$$P_{out} = P_m - P_{rot} \quad (10)$$

$$T_L = {}^{P_{out}}\!/_{\omega_r} \quad (11)$$

$$\omega_r = 2.\pi.Nr/60 \quad (12)$$

$$P_{in} = \sqrt{3}\,.V_{LL}.I_L.Cos\,\varphi \quad (13)$$

$$\eta = (P_{out}\,/P_{in})x100\% \quad (14)$$

where 'I_L' represents the line current, 'Cos φ' represents the power factor, 'V_{LL}' signifies the line-to-line voltage, and 'Nr' indicates the rotor speed (revolutions per minute).

3. METHOD

As part of the experimental study, the conventional and the new design of the three-phase induction motor were evaluated by running them at the Electrical Engineering Laboratory of the Institute of Technology Padang. The performance of both motors is assessed by analyzing the variations in the applied load relative to the alterations in each motor's coil current, output power, efficiency, speed, and torque. This method is used to assess the operational efficacy of the motors. All motor components are the same: the stator, rotor, pole quantity, coil type, stator slot quantity, and coil current specification. This study examines the operational parameters of the motor, specifically a 1 horsepower, 50 Hz, 380-volt, Y-connected motor featuring 1.8 amps, 2830 revolutions per minute, two poles, 18 slots, and a 0.55 mm coil with 118 turns per slot. The conventional motor utilizes a single-layer coil with 118 turns per slot. The coil of the new motor is designed with a two-layer arrangement, comprising two separate three-phase coil designs, each corresponding to its respective pole. This innovative coil design employs a 0.55 mm coil; each layer has an amount of 59, which means a total of 1 slot remains occupied by 118 turns, consistent with the traditional configuration. The new motor design incurs no supplementary expenditures.

Figure 1(a) illustrates the winding configuration in a conventional motor in its stator, featuring 18 slots and dual-pole arrangements. The coil arrangement comprises three coils (A, B, and C). The three-phase source must be connected to the input terminals (A1, B1, and C1) in a Y connection configuration, while terminals A2, B2, and C2 must be joined for optimal motor operation. Otherwise, the motor will function inefficiently. The stator coil design configuration for the novel design motor is illustrated in Figure 3. Coils A, B, C, D, E, and F comprise this design shape. The coil A1 (first coil) is initiated at slot number 2 on the initial layer, as illustrated in Figure 3(a). In contrast, the second layer (D1) initiates at slot number 4 (which has been displaced by 2 slots), as shown in Figure 3(b). In (5) illustrates that the spacing between each slot is 200 when a two-pole configuration is employed with 18 stator slots. This means that the form of the coil is like the 400-phase asymmetrical coil configuration of a 6-phase motor. To get the most out of the newly designed motor with a "Y" link, the coil configuration shown in Figure 3 needs to be connected in the way shown in Figure 4. In Figure 4, the terminals of coils A1, B1, and C1 are sequentially connected to the three-phase power supply (L1, L2, and L3).

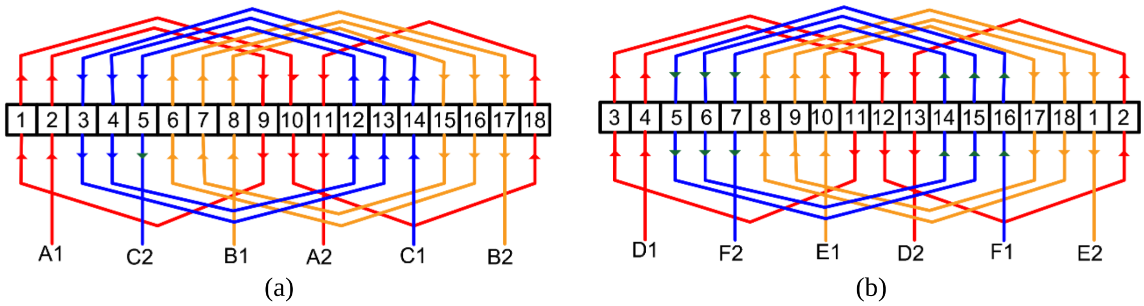

Figure 3. The stator coil of the new two-pole motor design has 18 slots, dispersed throughout the first (a) and second (b) layers

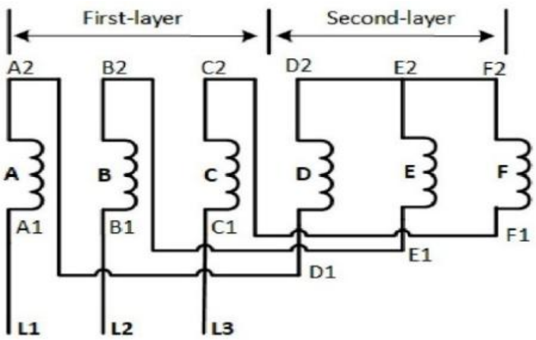

Figure 4. The arrangement of the coil connections of the new design motor, which adheres to the Y-connection standard

Figure 5 illustrates the process for testing an induction motor in a lab. A 3-phase induction motor is directly connected to a 1-phase induction generator, which is used to power several lamps as a load, as shown in Figure 5. A three-phase induction motor connected to a three-phase power source powers the induction generator. By altering the load on the induction generator that is directly connected to the motor, a three-phase induction motor is put through several tests. This enables the evaluation of the motor's performance under various circumstances and aids in determining its efficiency and operational limits. To measure current, voltage, power factor, frequency, and input power, a digital power meter is attached to the motor. An induction generator has a digital power meter that can measure output power, current, voltage, power factor, and frequency. Because the three-phase induction motor and the generator are directly connected, the generator's input power and the motor's output power are equal. The rotor speed is measured with a digital tachometer, then the motor efficiency and load torque are calculated using (10) to (14). A table and graph were then provided for analytical assessment based on the experimental results of the motors' performance.

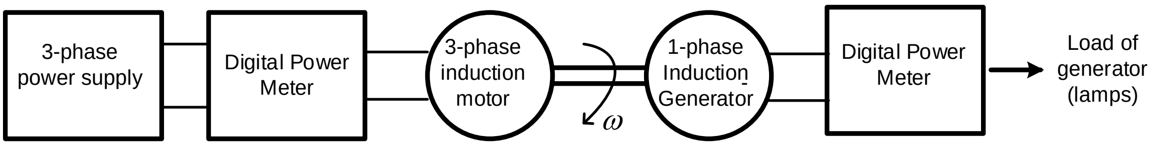

Figure 5. Procedure for measuring the performance of induction motors in a laboratory setting

4. RESULTS AND DISCUSSION

Laboratory testing was conducted on a newly developed 3-phase induction motor and a traditional 3-phase induction motor that was identical to the newly designed motor except for the winding configuration. The changes in current, speed, efficiency, and load torque were observed by varying the load on both motors. As shown in Figures 6 and 7 and Table 1, the performance results of both motors were then combined into a comparative graph and table. Figures 6 and 7 illustrate the efficiency (Eff(M40)), load torque (TL(M40)), rotor speed (Nr(M40)), and coil current (I(M40)) of the recently constructed 3-phase induction motor. Eff(M3), TL(M3), Nr(M3), and I(M3) stand for efficiency, load torque, rotor speed, and coil current, respectively, in a typical three-phase induction motor. Figure 6 shows that while the efficiency of the newly created motor consistently outperforms that of the conventional 3-phase induction motor (Figure 6(a)), the load torque is significantly higher (Figure 6(b)). The new motor design outperforms the traditional 3-phase induction motor in terms of efficiency (Eff) and load torque (TL), as shown in Figure 6 and Table 1. Table 1 shows that the 3-phase induction motor's upgraded design achieves an efficiency of 66.83%, but the conventional version only achieves 57.66%. The efficiency of the updated motor design has increased by 15.90%. The improved motor design results in a 16.05% increase in load torque, as Table 1 clearly shows. Figure 7 shows that the innovative motor design's velocity consistently surpasses that of the conventional 3-phase induction motor (Figure 7(a)), while the coil current is still relatively lower (Figure 7(b)).

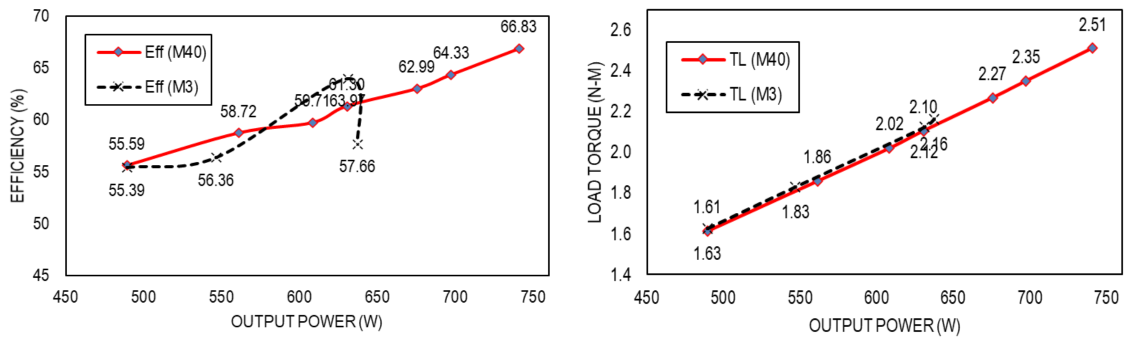

(a) (b)

Figure 6. The motors' characteristics include (a) their efficiency in relation to their output power and (b) their load torque in relation to their output power

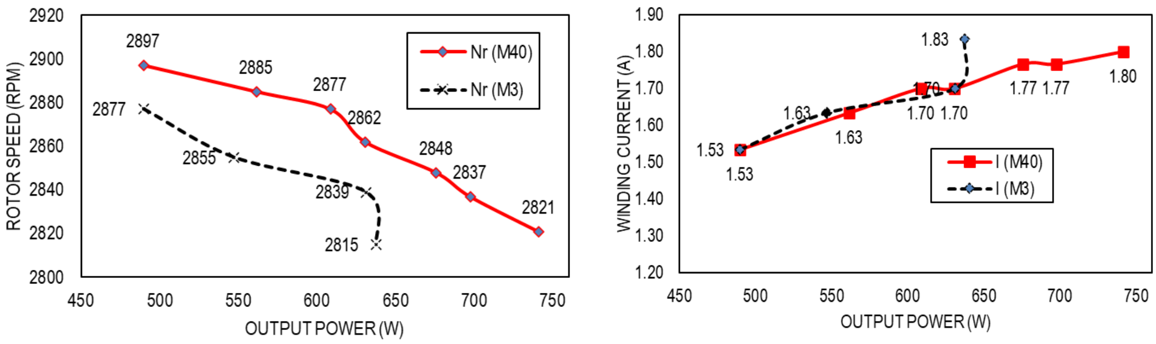

(a) (b)

Figure 7. Characteristics of output power include (a) rotor speed and (b) winding current

Figures 8 illustrate the fundamental winding distinctions between the traditional and the innovative motor design. Figure 8 shows that the color red represents the first layer coil, green signifies the second layer coil, and the symbol ‘τ’ denotes the coil’s pole pitch. Figures 8(a) and (b) delineate the differences between conventional and new motor designs, with the new one having an enlarged pole pitch (τ). Referencing (6) to (13), it is evident that augmenting the pole pitch ‘τ’ will enhance the magnetic flux (6). This augmentation subsequently elevates the EMF (7), rotor winding current (8), mechanical power (9), output power (10), load torque (11), and motor efficiency (14). Figures 6 and 7 present the graphical statistics that substantiate this assertion. The newly designed motor surpasses the conventional motor in overall performance.

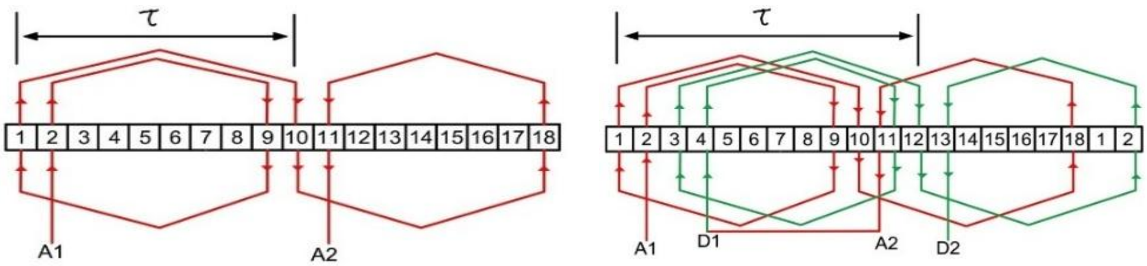

(a) (b)

Figure 8. The various arrangements of phase A 2-pole, 18-slot coil designs include (a) the coil arrangement in a conventional three-phase motor and (b) the coil arrangement in a new design motor

Table 1. Accomplishments of motor performance

Object	Proposed design	Old design	Enhancement (%)
Number of poles	2	2	0
Winding count per slot	118	118	0
Slot number	18	18	0
Output power (W)	741	637	16.29
Efficiency (%)	66.83	57.66	15.90
Speed of the rotor (RPM)	2821	2815	0.21
Load torque (Nm)	2.51	2.16	16.05
Winding current (A)	1.80	1.83	-1.82

The “Ansys Motor-CAD v2024.1.1” tool was used to model the coil designs for both motors to go along with the analysis. The “Ansys Motor-CAD” program was used to make the motor coil design shown in Figure 9. Figure 10 shows the results of models run with the same software. In Figure 9(a), you can see a modern three-phase induction motor coil design. In Figure 9(b), you can see an older three-phase induction motor coil design. As seen in Figure 10(a), the stator of the new design motor has a greater flux density in the air gap (0.2581 Tesla) than a regular motor, which only has 0.2344 Tesla (as seen in Figure 10(b)). It indicates that the newly designed motor has a higher flux density than a regular three-phase motor. As previously indicated, increasing flux density improves motor efficiency, speed, output power, and torque.

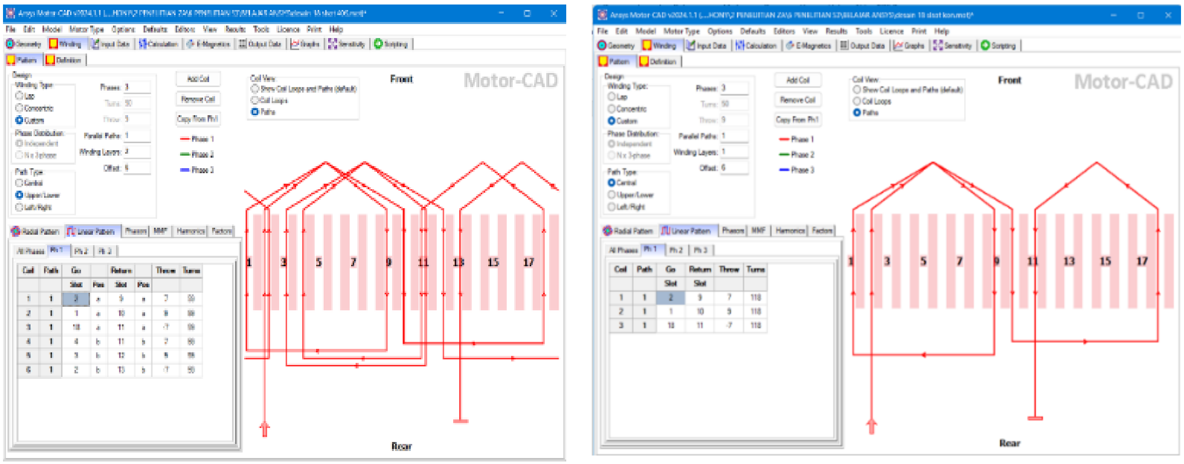

(a) (b)

Figure 9. Phase 1 (phase L1) coil illustrations for a three-phase induction motor, created using "Ansys Motor-CAD v2024.1.1," showing (a) the coil of a new three-phase motor and (b) the coil of a traditional three-phase motor

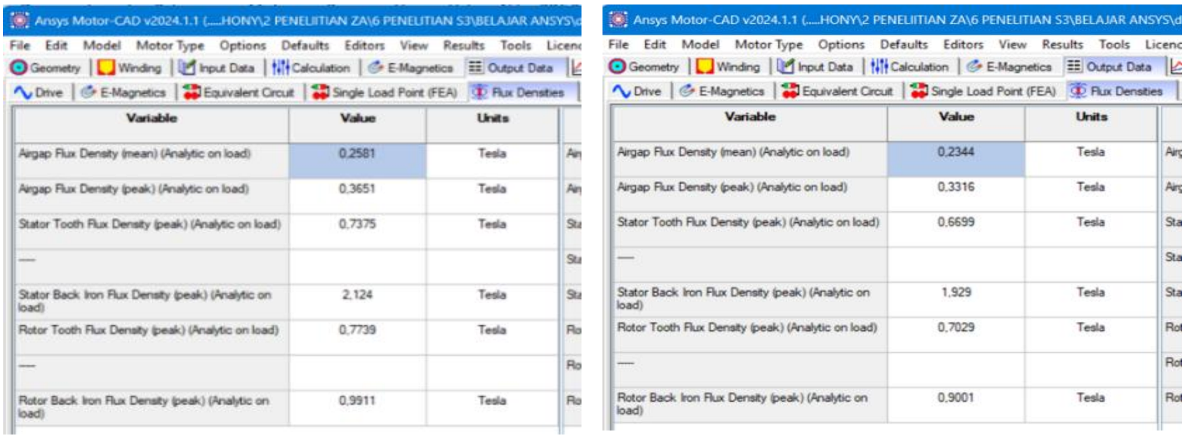

Variable	Value	Units
Airgap Flux Density (mean) (Analytic on load)	0.2581	Tesla
Airgap Flux Density (peak) (Analytic on load)	0.3651	Tesla
Stator Tooth Flux Density (peak) (Analytic on load)	0.7375	Tesla
—		
Stator Back Iron Flux Density (peak) (Analytic on load)	2.124	Tesla
Rotor Tooth Flux Density (peak) (Analytic on load)	0.7739	Tesla
—		
Rotor Back Iron Flux Density (peak) (Analytic on load)	0.9911	Tesla

Variable	Value	Units
Airgap Flux Density (mean) (Analytic on load)	0.2344	Tesla
Airgap Flux Density (peak) (Analytic on load)	0.3316	Tesla
Stator Tooth Flux Density (peak) (Analytic on load)	0.6699	Tesla
—		
Stator Back Iron Flux Density (peak) (Analytic on load)	1.929	Tesla
Rotor Tooth Flux Density (peak) (Analytic on load)	0.7029	Tesla
—		
Rotor Back Iron Flux Density (peak) (Analytic on load)	0.9001	Tesla

(a) (b)

Figure 10. Flux density results by using the "Ansys Motor-CAD v2024.1.1" tool, with data including (a) a new motor design and (b) a traditional motor design

Table 1 demonstrates that the new design motor's output power, efficiency, rotor speed, and load torque increase by 16.29%, 15.90%, 0.21%, and 16.05%, respectively, when compared to a traditional motor. The coil current of the new design motor is 1.82% less than that of a traditional motor. The performance gain is free because the new design of the three-phase induction motor uses the same stator, coil materials, and rotor as a traditional 3-phase induction motor (old design). Only a 3-phase induction motor with a 1 HP power capacity was used to evaluate the method described in this study; however, more research may lead to its development on 3-phase induction motors with bigger capacities.

5. CONCLUSION

The aim of this research is to develop a novel method for constructing a three-phase induction motor coil that enhances motor performance without incurring substantial cost increases. The study's findings indicate that the proposed coil design can significantly improve the overall performance of a three-phase induction motor without requiring substantial additional expenditures. The new coil design enhances the flux density of the motor, hence augmenting torque, speed, output power, and efficiency.

FUNDING INFORMATION

We sincerely thank everyone who helped make this research a reality. We sincerely appreciate Universitas Andalas' generous funding for this project, which was completed in compliance with research contract number 104/UN16.19/PT.01.03/PDD/2025.

AUTHOR CONTRIBUTIONS STATEMENT

This journal uses the Contributor Roles Taxonomy (CRediT) to recognize individual author contributions, reduce authorship disputes, and facilitate collaboration.

Name of Author	C	M	So	Va	Fo	I	R	D	O	E	Vi	Su	P	Fu
Zuriman Anthony	✓	✓	✓	✓	✓	✓	✓	✓	✓	✓	✓		✓	
Refdinal Nazir	✓	✓		✓	✓	✓	✓	✓		✓		✓		✓
Muhammad Imran Hamid		✓		✓	✓	✓	✓	✓		✓		✓		

C : **C**onceptualization
M : **M**ethodology
So : **So**ftware
Va : **Va**lidation
Fo : **Fo**rmal analysis
I : **I**nvestigation
R : **R**esources
D : **D**ata Curation
O : Writing - **O**riginal Draft
E : Writing - Review & **E**diting
Vi : **Vi**sualization
Su : **Su**pervision
P : **P**roject administration
Fu : **Fu**nding acquisition

CONFLICT OF INTEREST STATEMENT

The authors state no conflict of interest.

DATA AVAILABILITY

The authors confirm that the data supporting the findings of this study are available within the article [and/or its supplementary materials].

REFERENCES

[1] S. Zhao, X. Huang, Y. Fang, and H. Zhang, "DC-link-fluctuation-resistant predictive torque control for railway traction permanent magnet synchronous motor in the six-step operation," *IEEE Transactions on Power Electronics*, vol. 35, no. 10, pp. 10982–10993, Oct. 2020, doi: 10.1109/tpel.2020.2975497.

[2] S. Mahfoud, A. Derouich, N. El Ouanjli, N. V. Quynh, and M. A. Mossa, "A new hybrid ant colony optimization based PID of the direct torque control for a doubly fed induction motor," *World Electric Vehicle Journal*, vol. 13, no. 5, p. 78, Apr. 2022, doi: 10.3390/wevj13050078.

[3] Z. Yang, Q. Ding, X. Sun, J. Ji, and Q. Zhao, "Design and analysis of a novel wound rotor for a bearingless induction motor," *International Journal of Electronics*, vol. 106, no. 12, pp. 1829–1844, 2019, doi: 10.1080/00207217.2019.1625971.

[4] W. Pietrowski and K. Górny, "Analysis of torque ripples of an induction motor taking into account a inter-turn short-circuit in a stator winding," *Energies*, vol. 13, no. 14, p. 3626, 2020, doi: 10.3390/en13143626.

[5] J. Srinivasan, K. Selvaraj, J. Chitrarasu, and R. Resmi, "Design and analysis of squirrel cage induction motor in short pitch and full pitch winding configurations using FEA," Oct. 2016, doi: 10.1109/icett.2016.7873759.

[6] M. M. Tezcan and A. S. Akyurt, "Transforming of conventional type squirrel cage induction motor to permanent magnet synchronous motor for improving efficiency on industrial applications," *International Scientific and Vocational Studies Journal*, vol. 6, no. 1, pp. 32–40, 2022, doi: 10.47897/bilmes.1129634.

[7] R. Ni *et al.*, "Efficiency enhancement of general AC drive system by remanufacturing induction motor with interior permanent-magnet rotor," *IEEE Transactions on Industrial Electronics*, vol. 63, no. 2, pp. 808–820, Feb. 2016, doi: 10.1109/tie.2015.2477478.

[8] A. G. Yetgin, M. Turan, B. Cevher, A. İ. Çanakoğlu, and A. Gün, "Squirrel cage induction motor design and the effect of specific magnetic and electrical loading coefficient," *International Journal of Applied Mathematics Electronics and Computers*, vol. 7, no. 1, pp. 1–8, Mar. 2019, doi: 10.18100/ijamec.461795.

[9] A. Glowacz and Z. Glowacz, "Diagnosis of the three-phase induction motor using thermal imaging," *Infrared Physics & Technology*, vol. 81, pp. 7–16, Mar. 2017, doi: 10.1016/j.infrared.2016.12.003.

[10] A. Glowacz, "Acoustic based fault diagnosis of three-phase induction motor," *Applied Acoustics*, vol. 137, pp. 82–89, Aug. 2018, doi: 10.1016/j.apacoust.2018.03.010.

[11] A. M. Silva, F. J. T. E. Ferreira, M. V Cistelecan, and C. H. Antunes, "Multiobjective design optimization of generalized multilayer multiphase AC winding," *IEEE Transactions on Energy Conversion*, vol. 34, no. 4, pp. 2158–2167, Dec. 2019, doi: 10.1109/tec.2019.2935009.

[12] G. Joksimović, J. I. Melecio, P. M. Tuohy, and S. Djurović, "Towards the optimal 'slot combination' for steady-state torque ripple minimization: an eight-pole cage rotor induction motor case study," *Electrical Engineering*, vol. 102, no. 1, pp. 293–308, Nov. 2019, doi: 10.1007/s00202-019-00874-x.

[13] Z. Anthony, R. Nazir, and M. I. Hamid, "A review of strategies for improving 3-phase induction motor performance," *Andalasian International Journal of Applied Science, Engineering and Technology*, vol. 4, no. 1, pp. 01–12, Mar. 2024, doi: 10.25077/aijaset.v4i1.112.

[14] P. Sethupathi and N. Senthilnathan, “Comparative analysis of line-start permanent magnet synchronous motor and squirrel cage induction motor under customary power quality indices,” *Electrical Engineering*, vol. 102, no. 3, pp. 1339–1349, Feb. 2020, doi: 10.1007/s00202-020-00955-2.
[15] I. Gonzalez-Prieto, M. J. Duran, F. Barrero, M. Bermudez, and H. Guzman, “Impact of postfault flux adaptation on six-phase induction motor drives with parallel converters,” *IEEE Transactions on Power Electronics*, vol. 32, no. 1, pp. 515–528, Jan. 2017, doi: 10.1109/tpel.2016.2533719.
[16] H. S. Che, E. Levi, M. Jones, W.-P. Hew, and N. A. Rahim, “Current control methods for an asymmetrical six-phase induction motor drive,” *IEEE Transactions on Power Electronics*, vol. 29, no. 1, pp. 407–417, Jan. 2014, doi: 10.1109/tpel.2013.2248170.
[17] H. S. Che, M. J. Duran, E. Levi, M. Jones, W.-P. Hew, and N. A. Rahim, “Postfault operation of an asymmetrical six-phase induction machine with single and two isolated neutral points,” *IEEE Transactions on Power Electronics*, vol. 29, no. 10, pp. 5406–5416, Oct. 2014, doi: 10.1109/tpel.2013.2293195.
[18] I. Gonzalez-Prieto, I. Zoric, M. J. Duran, and E. Levi, “Constrained model predictive control in nine-phase induction motor drives,” *IEEE Transactions on Energy Conversion*, vol. 34, no. 4, pp. 1881–1889, Dec. 2019, doi: 10.1109/tec.2019.2929622.
[19] I. S. de Freitas *et al.*, “Twelve-phase induction machine analysis with harmonic injection,” in *2018 IEEE Energy Conversion Congress and Exposition (ECCE)*, 2018, pp. 1611–1618, doi: 10.1109/ecce.2018.8557360.
[20] M. J. Duran, I. Gonzalez-Prieto, N. Rios-Garcia, and F. Barrero, “A simple, fast, and robust open-phase fault detection technique for six-phase induction motor drives,” *IEEE Transactions on Power Electronics*, vol. 33, no. 1, pp. 547–557, Jan. 2018, doi: 10.1109/tpel.2017.2670924.
[21] M. A. Fnaiech, F. Betin, G.-A. Capolino, and F. Fnaiech, “Fuzzy logic and sliding-mode controls applied to six-phase induction machine with open phases,” *IEEE Transactions on Industrial Electronics*, vol. 57, no. 1, pp. 354–364, Jan. 2010, doi: 10.1109/tie.2009.2034285.
[22] J. K. Pandit, M. V Aware, R. V Nemade, and E. Levi, “Direct torque control scheme for a six-phase induction motor with reduced torque ripple,” *IEEE Transactions on Power Electronics*, vol. 32, no. 9, pp. 7118–7129, 2017, doi: 10.1109/tpel.2016.2624149.
[23] M. J. Duran, I. Gonzalez Prieto, M. Bermudez, F. Barrero, H. Guzman, and M. R. Arahal, “Optimal fault-tolerant control of six-phase induction motor drives with parallel converters,” *IEEE Transactions on Industrial Electronics*, vol. 63, no. 1, pp. 629–640, Jan. 2016, doi: 10.1109/tie.2015.2461516.
[24] A. Gautam, O. Ojo, M. Ramezani, and O. Momoh, “Computation of equivalent circuit parameters of nine-phase induction motor in different operating modes,” in *2012 IEEE Energy Conversion Congress and Exposition (ECCE)*, 2012, pp. 142–149, doi: 10.1109/ecce.2012.6342830.
[25] J. Rao, J. Xu, D. Z. Liu, X. D. Yang, X. P. Cui, and W. M. Ma, “Research of mathematical model of the twelve-phase linear induction motor with double-sided long stators,” *Applied Mechanics and Materials*, vol. 416–417, pp. 156–163, 2013, doi: 10.4028/www.scientific.net/amm.416-417.156.
[26] A. S. Abdel-Khalik, M. S. Abdel-Majeed, and S. Ahmed, “Effect of winding configuration on six-phase induction machine parameters and performance,” *IEEE Access*, vol. 8, pp. 223009–223020, 2020, doi: 10.1109/access.2020.3044025.
[27] Y. Demir and M. Aydin, “A novel dual three-phase permanent magnet synchronous motor with asymmetric stator winding,” *IEEE Transactions on Magnetics*, vol. 52, no. 7, pp. 1–5, 2016, doi: 10.1109/tmag.2016.2524027.
[28] Y. Demir and M. Aydin, “A novel asymmetric and unconventional stator winding configuration and placement for a dual three-phase surface PM motor,” *IEEE Transactions on Magnetics*, vol. 53, no. 11, pp. 1–5, Nov. 2017, doi: 10.1109/tmag.2017.2710424.
[29] J. Paredes, B. Prieto, M. Satrustegui, I. Elosegui, and P. Gonzalez, “Improving the performance of a 1-MW induction machine by optimally shifting from a three-phase to a six-phase machine design by rearranging the coil connections,” *IEEE Transactions on Industrial Electronics*, vol. 68, no. 2, pp. 1035–1045, Feb. 2021, doi: 10.1109/tie.2020.2969099.
[30] P. Giangrande, V. Madonna, S. Nuzzo, and M. Galea, “Design of fault-tolerant dual three-phase winding PMSM for helicopter landing gear EMA,” in *2018 IEEE International Conference on Electrical Systems for Aircraft, Railway, Ship Propulsion and Road Vehicles & International Transportation Electrification Conference (ESARS-ITEC)*, Nov. 2018, pp. 1–6, doi: 10.1109/esars-itec.2018.8607684.
[31] A. S. Abdel-Khalik, A. M. Massoud, and S. Ahmed, “Application of standard three-phase stator frames in prime phase order multiphase machine construction,” *IEEE Transactions on Industrial Electronics*, vol. 66, no. 4, pp. 2506–2517, Apr. 2019, doi: 10.1109/tie.2018.2840497.
[32] J. Laksar, R. Cermak, and K. Hruska, “Challenges in the electromagnetic design of multiphase machines: winding and equivalent circuit parameters,” *Energies*, vol. 14, no. 21, p. 7335, Nov. 2021, doi: 10.3390/en14217335.
[33] B. M. Dinh, “Efficiency improvement of squirrel cage induction motor by rotor slot designs,” Mar. 2023, doi: 10.46254/an13.20230184.
[34] Z. Zulkarnaini, S. Bandri, E. Erhaneli, Z. Anthony, Y. Warmi, and A. Y. D. Rachman, “Enhance the performance of 3-phase induction motors with the utilization of a 9-phase winding design,” *International Journal of Power Electronics and Drive Systems (IJPEDS)*, vol. 16, no. 3, p. 1528, 2025, doi: 10.11591/ijpeds.v16.i3.pp1528-1536.
[35] A. Selema, M. N. Ibrahim, and P. Sergeant, “Electrical machines winding technology: latest advancements for transportation electrification,” *Machines*, vol. 10, no. 7, p. 563, 2022, doi: 10.3390/machines10070563.
[36] A. M. Silva, F. J. T. E. Ferreira, G. Falcao, and M. Rodrigues, “Novel method to minimize the air-gap MMF spatial harmonic content in three-phase windings,” in *2018 XIII International Conference on Electrical Machines (ICEM)*, 2018, pp. 2504–2510, doi: 10.1109/icelmach.2018.8507206.
[37] J. Chen, Y. Fujii, M. W. Johnson, A. Farhan, and E. L. Severson, “Optimal design of the bearingless induction motor,” *IEEE Transactions on Industry Applications*, vol. 57, no. 2, pp. 1375–1388, Mar. 2021, doi: 10.1109/tia.2020.3044970.
[38] S. I. Suriano-Sánchez, M. Ponce-Silva, V. H. Olivares-Peregrino, and S. E. De León-Aldaco, “A review of torque ripple reduction design methods for radial flux PM motors,” *Eng*, vol. 3, no. 4, pp. 646–661, Dec. 2022, doi: 10.3390/eng3040044.
[39] S. M. S. H. Rafin, Q. Ali, S. Khan, and T. A. Lipo, “A novel two-layer winding topology for sub-harmonic synchronous machines,” *Electrical Engineering*, vol. 104, no. 5, pp. 3027–3035, Mar. 2022, doi: 10.1007/s00202-022-01531-6.
[40] S. El Daoudi, L. Lazrak, N. El Ouanjli, and M. Ait Lafkih, “Improved DTC-SPWM strategy of induction motor by using five-level POD-PWM inverter and MRASSF estimator,” *International Journal of Dynamics and Control*, vol. 9, no. 2, pp. 448–462, 2020, doi: 10.1007/s40435-020-00667-2.
[41] S. Mahfoud, A. Derouich, N. EL Ouanjli, M. EL Mahfoud, and M. Taoussi, “A new strategy-based PID controller optimized by genetic algorithm for DTC of the doubly fed induction motor,” *Systems*, vol. 9, no. 2, p. 37, May 2021, doi: 10.3390/systems9020037.

[42] W. Pei, Q. Zhang, and Y. Li, "Efficiency optimization strategy of permanent magnet synchronous motor for electric vehicles based on energy balance," *Symmetry*, vol. 14, no. 1, p. 164, Jan. 2022, doi: 10.3390/sym14010164.
[43] F. Edition and S. J. Chapman, "Electric machinery fundamentals," *4th ed. New York: McGraw-Hill*, 2005. www.mhhe.oom.
[44] J. F. Gieras, "Electrical machines : fundamentals of electromechanical energy conversion," *1st ed. Boca Raton: Boca Raton London New York CRC Press*, 2017.

BIOGRAPHIES OF AUTHORS

Zuriman Anthony is a lecturer in the Department of Electrical Engineering at the Institute of Technology Padang (ITP), Padang, Indonesia. He received his B.E. in electrical engineering from Padang Institute of Technology, Padang, Indonesia, in 1996. He received the M.Eng. degree in electrical engineering from Gadjah Mada University, Yogyakarta, Indonesia, in 2002. He has always been active in various research activities, especially in the fields of electrical machines and electrical power systems. He is currently completing a doctoral program in the electrical engineering department at Universitas Andalas, Padang, Indonesia. His areas of interest are energy conversion, electrical machines, and electrical power system analysis. He can be contacted at email: zuriman@itp.ac.id.

Refdinal Nazir is a lecturer in the Electrical Engineering Department at the Universitas Andalas, Indonesia. Refdinal Nazir received his B.E. and M.Tech. degrees in Electrical Engineering from the Bandung Institute of Technology (ITB) in Bandung, Indonesia, in 1985 and 1986, respectively. He received a Ph.D. degree from the University of Technology Malaysia (UTM), Johor Bahru, Malaysia, in 1999. He has some experience in solving energy modelling and planning problems using LEAP, HOMER, and RETScreen software. He has published several papers at various national and international conferences and has done a number of in-house and industry projects. His areas of interest are electric machines, electric power and energy, renewable energy sources, microgrids, energy conservation, and energy efficiency. He can be contacted at email: refdinalnazir@eng.unand.ac.id.

Muhammad Imran Hamid is a lecturer in the Electrical Engineering Department at Universitas Andalas in Indonesia. Muhammad Imran Hamid received his B.E. in electrical engineering from Hasanuddin University in 1996. He received the M.Eng. degree in Electrical Engineering from the Bandung Institute of Technology in 2001. He received a Ph.D. degree from the Universiti Teknologi Malaysia in 2014. His areas of interest are renewable energy, power electronics, and power quality. He can be contacted at email: imran@eng.unand.ac.id.